J|A|C|S
ARTICLES
Published on Web 06/12/2002

Symmetry-Breaking Phenomena in Metalloporphyrin π-Cation Radicals

Torgil Vangberg, Renate Lie, and Abhik Ghosh*

Contribution from the Department of Chemistry, Faculty of Science, University of Tromsø, N-9037 Tromsø, Norway

Received June 11, 2001

Abstract: Density functional theory (DFT) calculations of the energetics, molecular structures, and spin density profiles of metalloporphyrin π-cation radicals suggest that the common practice of describing these radicals in terms of a universal A_{1u}/A_{2u} dichotomy is often not justified, confirming a possibility first foreseen by Prendergast and Spiro (ref 15) over a decade ago on the basis of vibrational spectroscopy and semiempirical calculations. Because of near-degeneracy of the a_{1u} and a_{2u} HOMOs of many metalloporphyrins, the cation radicals derived from these compounds undergo a pseudo-Jahn−Teller (pJT) distortion and are, therefore, best described as ^2A_u with reference to the C_{4h} point group, rather than as $^2A_{1u}$ (D_{4h}) or $^2A_{2u}$ (D_{4h}). We find that the porphyrin cation radicals undergo a pJT distortion if the energy difference between the $^2A_{1u}$ and $^2A_{2u}$ π-cation radicals, optimized under D_{4h} symmetry constraints, is less than 0.15 eV. According to this criterion, metallo-porphine and metallo-OEP π-cation radicals should always be pJT-distorted and metallo-*meso*-tetrahalogenoporphyrin radicals should not. For $[Zn(TPP^{\bullet})]^+$, the $^2A_{1u}/^2A_{2u}$ energy difference is almost exactly at the threshold of 0.15 eV, consistent with the experimental observation of both symmetry-broken and undistorted structures for this species. The $^2A_{1u}/^2A_{2u}$ energy difference (when the molecular geometries are optimized under a D_{4h} symmetry constraint) also appears to govern whether the real pJT-distorted cation radical is more A_{1u}- or A_{2u}-like in terms of its spin density profile. Because many metalloporphyrin π-cation radicals exist as cofacial dimers in the crystalline phase, we examined the symmetries and structures of the model compounds $[\{Zn(P)\}_2]^{+,2+}$ by means of DFT geometry optimizations. The results showed that dimerization has relatively little impact on the bond length alternation in the individual rings. A final interesting result, consistent with experiment, is that the bond length alternation in the delocalized mixed-valence dimer $[\{Zn(P)\}_2]^+$ is about half that found for $[\{Zn(P)\}_2]^{2+}$.

Introduction

Few classes of molecules have elicited as much scrutiny and controversy in recent decades as the Compound I intermediates of peroxidases, catalases, and their synthetic models.[1−7] These intermediates are two oxidation equivalents above iron(III) and, in general, may be described as iron(IV)-oxo porphyrin π-cation radicals. While the +4 oxidation state of the iron center appears to be on firm ground, a frustrating controversy has surrounded the nature of the porphyrin radical of the horseradish peroxidase Compound I (HRP-I).[1−7] In a review on resonance Raman spectra of highly oxidized metalloporphyrins and heme proteins, Kitagawa and Mizutani[6] describe this controversy as "vexing," a description echoed by Terner et al.[2] in his more recent review. The reason for this controversy is that the two HOMOs[8] of the porphyrin ligand, which transform as a_{1u} and a_{2u} in a D_{4h} metalloporphyrin, are very nearly degenerate and the relative stability of the A_{1u}- and A_{2u}-type cation radicals depends sensitively on the nature of the peripheral substituents and other factors.[9] For synthetic metalloporphyrins, a large body of EPR,[10] NMR,[11] resonance Raman,[12,13] and theoretical[14] results have led to a simple rule of thumb with regard to this issue: metallo-OEP-type (OEP, β-octaethylporphyrin) derivatives form A_{1u}-type cation radicals while metallo-TPP (TPP, *meso*-tetraphenylporphyrin) derivatives form A_{2u}-type cation radicals. This can

* Corresponding author. E-mail: abhik@chem.uit.no.

(1) Weiss, R.; Gold, A.; Trautwein, A. X.; Terner, J. In *The Porphyrin Handbook*; Kadish, K. M., Smith, K. M., Guilard, R., Eds.; Academic: New York, 2000; Vol. 4, Chapter 29, pp 65−96.
(2) Terner, J.; Gold, A.; Weiss, R.; Mandon, D.; Trautwein, A. X. *J. Porphyrins Phthalocyanines* **2001**, *5*, 357.
(3) Hosten, C. M.; Sullivan, A. M.; Palaniappan, V.; Fitzgerald, M. M.; Terner, J. *J. Biol. Chem.* **1994**, *269*, 13966.
(4) Palaniappan, V.; Terner, J. *J. Biol. Chem.* **1989**, *264*, 16046.
(5) Kincaid, J. R.; Zheng, Y.; Al-Mustafa, J.; Czarnecki, K. *J. Biol. Chem.* **1996**, *271*, 28805.
(6) Kitagawa, T.; Mizutani, Y. *Coord. Chem. Rev.* **1994**, *135*, 685−735.
(7) Kincaid, J. R. In *The Porphyrin Handbook*; Kadish, K. M., Smith, K. M., Guilard, R., Eds.; Academic: New York, 2000; Vol. 7, Chapter 51, pp 225−292.
(8) Gouterman, M. In *The Porphyrins*; Dolphin, D., ed; Academic: New York, 1978, Vol. III, Part A, Chapter 1.
(9) For a recent account, see: Ghosh, A. *J. Am. Chem. Soc.* **1995**, *117*, 4691
(10) Fajer, J.; Davis, M. S. In *The Porphyrins*; Dolphin, D., Ed.; Academic: New York, 1978; Vol. III, Part A, Physical Chemistry, Chapter 4, pp 197−256.
(11) Walker, F. A. In *The Porphyrin Handbook*; Kadish, K. M., Smith, K. M., Guilard, R., Eds.; Academic: New York, 2000; Vol 5, Chapter 36, pp 81−183.
(12) Czernuszewicz, R.; Macor, K. A.; Li, X.-Y.; Kincaid, J. R.; Spiro, T. G. *J. Am. Chem. Soc.* **1989**, *111*, 3860.
(13) Oertling, W. A.; Salehi, A.; Chang, C. K.; Babcock, G. T. *J. Phys. Chem.* **1989**, *93*, 1311.
(14) Spellane, P. J.; Gouterman, M.; Antipas, A.; Kim, S.; Liu, Y. C. *Inorg. Chem.* **1980**, *19*, 386.

10.1021/ja011438h CCC: $22.00

be readily rationalized in molecular orbital terms.[14] Electron-donating substituents at the β-positions, where the a_{1u} orbital has significant amplitude but not the a_{2u} orbital, should destabilize the a_{1u} orbital and favor the formation of A_{1u} radicals. Similarly, electron-donating substituents at the meso positions, where the a_{2u} orbital has significant amplitude but not the a_{1u} orbital, should destabilize the a_{2u} orbital and favor the formation of A_{2u}-type cation.

Interestingly, the porphyrin literature offers a number of hints that the above rule of thumb is simplistic. As discussed by Prendergast and Spiro over a decade ago,[15] a common scenario is that the a_{1u} and a_{2u} HOMOs of a porphyrin are very nearly degenerate and, consequently, a cation radical derived from this porphyrin is expected to be unstable with respect to an a_{2g} ($a_{1u} \times a_{2u}$) pseudo-Jahn−Teller (pJT) distortion. Experimental results appeared to be in general agreement with this proposition. Thus, Song, Reed, and Scheidt reported a crystallographic determination of $[Zn(OEP^{\bullet})]^+$ that revealed a "striking alternation of bond lengths around the 16-membered inner ring" consistent with an a_{2g} ($a_{1u} \times a_{2u}$) pJT distortion.[16,17] Second, resonance Raman spectroscopy has shown that certain metalloporphyrin cation radicals have markedly lower a_{2g} vibrational frequencies than their (neutral) nonradical precursors.[15] Third, the ESR spin density profiles of metallo-OEP radicals, often considered the prototype of A_{1u} radicals, actually cannot be interpreted in terms of a pure a_{1u}-type spin density distribution; it is essential to invoke a certain amount of a_{1u}/a_{2u} mixing.[10] Using semiempirical molecular orbital calculations, Prendergast and Spiro[15] presented a theoretical framework that satisfactorily explained these observations and, in particular, successfully obtained theoretical pJT-distorted π-cation radical geometries. Finally, a few recent papers also invoke A_{1u}/A_{2u} mixed states to explain specific spectroscopic features of metalloporphyrin π-cation radicals.[18,19] In this paper, we revisit this subject, using density functional theory (DFT) calculations.

Two major, albeit interrelated, considerations led us to undertake this study.

First, despite enormous progress in computational chemistry over the past decade, the semiempirical study by Prendergast and Spiro[15] continues to serve as the only significant theoretical treatment of the question of pJT distortions in metalloporphyrin π-cation radicals. This is not a satisfactory situation because over the past decade, it has become clear that semiempirical and ab initio Hartree−Fock calculations do not provide even a qualitatively correct description of the potential energy surfaces of porphyrin-type molecules.[20] As may be verified by frequency analyses, the minimum-energy structures of *neutral* (i.e. nonradical) porphyrin-type molecules at these levels of theory correspond to frozen resonance forms with localized single and double bonds instead of realistic delocalized structures.[20] These problems are corrected when electron correlation is suitably accounted for, either explicitly via MP2,[20] CASPT2,[21] and other correlated ab initio methods or implicitly via DFT.[20,22−24] We have shown, for instance, that semiempirical calculations have resulted in an "incorrect" ordering of the relative stabilities of different metalloporphyrin isomers, relative to DFT calculations.[25] To resolve the question of pJT distortions in metalloporphyrin π-cation radicals with greater certainty, we chose to reinvestigate the problem with nonlocal DFT, the best contemporary quantum chemical approach that is readily applicable to molecules the size of substituted porphyrins.[23,24]

Second, despite the total absence of theoretical studies on the potential energy surfaces of metalloporphyrin π-cation radicals over the past decade, a vast body of crystallographic work[26−39] on these species has accumulated in recent years. A main goal of this study is to provide a theoretical analysis of this large body of structural data.[26] Scheidt and co-workers have reported a series of X-ray crystallographic studies on metalloporphyrin π-cation radicals, many of which do reveal a significant bond length alternation around the central 16-membered $C_{12}N_4$ ring.[26] However, because these alternant structures were first observed in π-cation radicals that exist as cofacial dimers in the crystalline phase, Scheidt raised the possibility that the observed bond length alternations may result from the "dimerization" rather than from a pJT distortion.[26] Recently, Scheidt and co-workers have also detected significant bond length alternation in "monomeric" π-cation radical systems where sterically hindering substituents preclude significant interring interaction.[26,38] Unfortunately, not all π-cation radicals studied by Scheidt and co-workers exhibited an alternant structure and certain structures were simply ambiguous, apparently exhibiting bond length alternation for only part of the porphyrin ring.[26] In his recent review,[26] Scheidt has written: "The general difficulty with this pJT distortion explanation, as for all Jahn−Teller systems, is the lack of any predictive power as to whether the phenomenon will actually be seen. ... The final question concerning bond alternation pattern ... : Do all π-cation derivatives have it? My personal conclusion is that not all derivatives satisfy the conditions for its presence. Definitive evidence, pro or con, cannot come solely from structural studies." Overall, while calling pJT distortions the

(15) Prendergast, K.; Spiro, T. G. *J. Phys. Chem.* **1991**, *95*, 9728.
(16) Song, H. S.; Orosz, R. D.; Reed, C. A.; Scheidt, W. R. *Inorg. Chem.* **1990**, *29*, 4274.
(17) Song, H.; Reed, C. A.; Scheidt, W. R. *J. Am. Chem. Soc.* **1989**, *111*, 6867.
(18) Kalsbeck, W. A.; Seth, J.; Bocian, D. F. *Inorg. Chem.* **1996**, *35*, 7935.
(19) Jayaraj, K.; Terner, J.; Gold, A.; Roberts, D. A.; Austin R. N.; Mandon, D.; Weiss, R.; Bill, E.; Muther, M.; Trautwein, A. X. *Inorg. Chem.* **1996**, *35*, 1632
(20) Almlöf, J.; Fischer, T. H.; Gassman, P. G.; Ghosh, A.; Häser, M. *J. Phys. Chem.* **1993**, *97*, 10964.
(21) Merchan, M.; Orti, E.; Roos, B. O. *Chem. Phys. Lett.* **1994**, *221*, 136.
(22) Song, H.; Reed, C. A.; Scheidt, W. R. *J. Am. Chem. Soc.* **1989**, *111*, 6867.
(23) For a review of DFT calculations on porphyrins, see: Ghosh, A. *Acc. Chem. Res.* **1998**, *31*, 189.
(24) For another review of DFT calculations on porphyrins, see: Ghosh, A. In *The Porphyrin Handbook*; Kadish, K. M., Ed.; Academic: New York, 2000; Vol. 7, Chapter 47, p 1.
(25) Ghosh, A.; Vangberg, T. *Inorg. Chem.* **1998**, *37*, 6276.
(26) Scheidt, W. R. *J. Biol. Inorg. Chem.* **2001**, *6*, 727.
(27) Erler, B. S.; Scholz, W. F.; Lee, Y. J.; Scheidt, R. W.; Reed, C. A. *J. Am. Chem. Soc.* **1987**, *109*, 2644.
(28) Song, H.; Rath, N. P.; Reed, C. A.; Scheidt, W. R. *Inorg. Chem.* **1989**, *28*, 1839.
(29) Renner, M. W.; Barkigia, K. M.; Zhang, Y.; Medforth, C. J.; Smith, K. M.; Fajer, J. *J. Am. Chem. Soc.* **1994**, *116*, 8582.
(30) Gans, P.; Buisson, G.; Duée, E.; Marchon, J.-C.; Erler, B. S.; Scholz, W. F.; Reed, C. A. *J. Am. Chem. Soc.* **1986**, *108*, 1223.
(31) Gupta, G. P.; Lang, G.; Lee, Y. J.; Scheidt, W. R.; Shelly, K.; Reed, C. A. *Inorg. Chem.* **1987**, *26*, 3022.
(32) Barkigia, K. M.; Spaulding, L. D.; Fajer, J. *Inorg. Chem.* **1983**, *9*, 349.
(33) McGhee, E. M.; Godfrey, M. R.; Hoffman, B. M.; Ibers, J. A. *Inorg. Chem.* **1991**, *30*, 803.
(34) Schulz, C. E.; Song, H. S.; Mislankar, A.; Orosz, R. D.; Reed, C. A.; Debrunner, P. G.; Scheidt, W. R. *Inorg. Chem.* **1997**, *36*, 406.
(35) Brancato-Buentello, K. E.; Scheidt, W. R. *Angew. Chem., Int. Ed. Engl.* **1997**, *36*, 1456.
(36) Scheidt, W. R.; Song, H. S.; Haller, K. J.; Safo, M. K.; Orosz, R. D.; Reed, C. A.; Debrunner, P. G.; Schulz, C. E. *Inorg. Chem.* **1992**, *31*, 939.
(37) Scheidt, W. R.; Brancato-Buentello, K. E.; Song, H. S.; Reddy, K. V.; Cheng, B. S. *Inorg. Chem.* **1996**, *35*, 7500.
(38) Ehlinger, N.; Scheidt, W. R. *Inorg. Chem.* **1999**, *38*, 1316.
(39) Spaulding, L. D.; Eller, P. G.; Bertrand, J. A.; Felton, R. H. *J. Am. Chem. Soc.* **1974**, *96*, 982.

"most coherent explanation" of the observed structural features, Scheidt emphasizes the subtlety and ambiguity of the experimental scenario.[26]

To summarize, this study aims to answer the following questions:

(a) How accurately (as judged, for example, by comparison with gas-phase photoelectron spectra) does DFT describe the energetics of ionized states of porphyrins?

(b) Are the pJT distortions proposed by Prendergast and Spiro real?

(c) Do the alternant structures observed crystallographically reflect pJT distortions?

(d) For which specific metallporphyrin π-cation radicals are pJT distortions expected?

(e) How are pJT distortions affected by cofacial dimer formation?

We have addressed these questions using nonlocal density functional theory (DFT) calculations.[23,24]

Methods

Unless otherwise mentioned, all calculations were carried out with the ADF program,[40−44] using versions 2.3, 1999, and 2000.02. Because of minor differences among the three versions, relative energies were always computed by using the same version of the program. We used Slater-type triple-ζ plus polarization basis sets (the basis sets denoted as IV in the program manual), the Perdew−Wang 1991 nonlocal functional,[45] and a fine integration grid (5.0) in all calculations. The convergence criteria used in the geometry optimizations were 10^{-4} hartree for the energy, 10^{-3} hartree/Å for the gradients, and 5×10^{-3} Å for the coordinates. Unless otherwise mentioned, all calculations were spin-restricted.

Neutral and ionized states of the following compounds were studied: porphine derivatives, M(P) (M = H_2, Ni, Zn); *meso*-tetra(phenyl)porphyrin derivatives, M(TPP) (M = H_2, Ni, Zn); β-octaethylporphyrin derivatives, M(OEP) (M = H_2, Ni, Zn, Mg); magnesium *meso*-tetra(methyl)porphyrin, Mg(TMP); zinc *meso*-tetra(X)porphyrin, Zn(TXP) (X = F, Br); zinc *meso*-tetrakis(2,6-dichlorophenyl)porphyrin, Zn(TDCPP); *meso*-tetrakis(pentafluorophenyl)porphyrin, M(TPFPP) (M = Ni, Zn); and zinc β-octa(X)porphyrin derivatives, Zn(OXP) (X = F, Cl, Br). The optimized Cartesian coordinates of most of the molecules studied are listed in the Supporting Information.

Results and Discussion

(a) Energetics of Metalloporphyrin Cations and Comparison with Photoelectron Spectra. At present, DFT is probably the only "practical" high-quality quantum chemical method capable of dealing with the large molecules of interest in this study. In addition, we have found that DFT provides an excellent description of the energetics of the gas-phase photoelectron spectra and hence of the low-lying ionized states of free-base porphine.[46] Before embarking on the subtle issue of pJT distortions in metalloporphyrin cation radicals, we wished to extend the available evidence with regard to the performance of DFT in calculations of the energetics of ionized states (i.e. ionization potentials, IPs) of porphyrins. Table 1 presents a collection of DFT(PW91/TZP) ΔSCF vertical IPs, along with the corresponding experimental[47] values, where available. The calculated and the eight available experimental IPs agree quantitatively, with a mean deviation of only 0.08 eV between theory and experiment. DFT clearly provides an excellent description of the energetics of the ionized states of porphyrins.

Table 1. Vertical DFT(PW91/TZP) ΔSCF IPs (eV) of Selected Porphyrins, with Eight Experimentally Available IPs Shown in Bold for Comparison[a]

		IP		
molecule	point group	first	second	third
$(P)H_2$[b]	D_{2h}	6.99 ($^2B_{1u}$)	7.17 (^2A_u)	7.93 ($^2B_{2g}$)
		6.9[b]	**7.1**[b]	**8.1**[b]
Zn(P)	D_{4h}	7.04 ($^2A_{2u}$)	7.10 ($^2A_{1u}$)	
Ni(P)	D_{4h}	7.09 ($^2A_{1u}$)	7.12 ($^2A_{2u}$)	
$(OEP)H_2$	D_{2h}	6.22 ($^2B_{1u}$)	6.40 (^2A_u)	
		6.24[c]	6.49[c]	
Zn(OEP)	D_{4h}	6.16 ($^2A_{1u}$)	6.24 ($^2A_{2u}$)	
		6.18[c]		
Ni(OEP)	D_{4h}	6.20 ($^2A_{2u}$)	6.21 ($^2A_{1u}$)	
$(TPP)H_2$	D_{2h}	6.52 ($^2B_{1u}$)	6.77 (^2A_u)	7.43 ($^2B_{2g}$)
		6.43[c]	**6.70**[c]	
Zn(TPP)	D_{4h}	6.57 ($^2A_{2u}$)	6.72 ($^2A_{1u}$)	7.43 ($^2B_{2g}$)

[a] The calculated vertical IPs reported in this table are not directly comparable with the adiabatic IPs in Table 2 because the IPs in the two tables were obtained with slightly different versions of the ADF program system. [b] Reference 46. [c] Reference 47.

The lowest ionized states of the TPP derivatives correspond to A_{2u}-type π-cation radicals, consistent with commonly accepted ideas[14] in the porphyrin field. However, our finding that the lowest vertical IPs of $(OEP)H_2$ and Ni(OEP) (Table 1) correspond to A_{2u}-type π-cation radicals does not agree with accepted ideas[14] and, in the case of $(OEP)H_2$, constitutes a reassignment of the experimental photoelectron spectrum.[32] [Note: The $^2B_{1u}$ (D_{2h} notation) ground state of $(OEP)H_2^{+\bullet}$ corresponds to an A_{2u}-type (D_{4h} notation) π-cation radical.] One can of course argue that the DFT calculations result in a wrong assignment; however, the close agreement between the DFT and experimental IPs, in our opinion, should not be casually dismissed. Indeed, from our personal viewpoint, this somewhat disturbing reassignment of the photoelectron spectrum of $(OEP)H_2$[47] derivatives is what ultimately led us to undertake a careful examination of the energetics and structures of metalloporphyrin π-cation radicals, i.e., the subject matter of this paper. Having validated the performance of DFT with regard to the energetics of the ionized states of metalloporphyrins, we shall not have much further to say about photoelectron spectra and shall proceed to discuss the structural aspects of these species.

We shall see later that metallo-OEPs provide some of the most clear-cut examples of pJT distortions, both experimentally[26] and in our computational studies. We shall also see that the spin density profiles of pJT-distorted metallo-OEP radicals are more A_{1u}-like than A_{2u}-like, consistent with generally accepted ideas.[14]

(b) The Energetics of pJT Distortions. The energetics of the pJT distortions was evaluated in the following way. For each porphyrin, the geometry was optimized with the highest possible symmetry constraint, usually D_{4h}, for the neutral state and for the $^2A_{1u}$ and $^2A_{2u}$ cation radicals. Another set of

(40) The ADF program is obtainable from the following: Scientific Computing and Modelling, Department of Theoretical Chemistry, Vrije Universiteit, De Boelelaan 1083, 1081 HV Amsterdam, The Netherlands.
(41) Versluis, L.; Ziegler, T. *J. Chem. Phys.* **1988**, *88*, 322.
(42) te Velde, G.; Baerends, E. J. *J. Comput. Phys.* **1992**, *99*, 84.
(43) Guerra, C. F.; Snijders, J. G.; teVelde, G.; Baerends, E. J. *Theor. Chem. Acc.* **1998**, *99*, 391.
(44) Baerends, E. J.; Ellis, D. E.; Ros, P. *Chem. Phys.* **1973**, *2*, 41.
(45) Perdew, J. P.; Chevary, J. A.; Vosko, S. H.; Jackson, K. A.; Pederson, M. R.; Singh, D. J.; Fiolhais, C. *Phys. Rev. B* **1992**, *46*, 6671.
(46) Ghosh, A.; Vangberg, T. *Theor. Chem. Acc.* **1997**, *97*, 143.
(47) Gruhn, N. E.; Lichtenberger, D. L.; Ogura, H.; Walker, F. A. *Inorg. Chem.* **1999**, *38*, 4023.

Table 2. Adiabatic DFT(PW91/TZP) IPs (eV) of Porphyrins[a]

molecule	point group	IP lowest	IP second lowest	bond length alternation
Zn(P)	D_{4h}	6.91 ($^2A_{2u}$)	6.96 ($^2A_{1u}$)	
	C_{4h}	6.89 (^2A_u)		yes
Ni(P)	D_{4h}	6.96 ($^2A_{1u}$)	7.00 ($^2A_{2u}$)	
	C_{4h}	6.95 (^2A_u)		yes
Zn(TFP)	D_{4h}	6.98 ($^2A_{2u}$)	7.55 ($^2A_{1u}$)	
	C_{4h}	6.98 (^2A_u)		no
Zn(TBrP)	D_{4h}	6.97 ($^2A_{2u}$)	7.48 ($^2A_{1u}$)	
	C_{4h}	6.97 (^2A_u)		no
Zn(OEP)	D_{4h}	6.13 ($^2A_{2u}$)	6.18 ($^2A_{1u}$)	
	C_{4h}	6.12 (^2A_u)		yes
Ni(OEP)	D_{4h}	6.17 ($^2A_{1u}$)	6.17 ($^2A_{2u}$)	
	C_{4h}	6.13 (^2A_u)		yes
Mg(OEP)	D_{4h}	6.17 ($^2A_{2u}$)	6.26 ($^2A_{1u}$)	
	C_{4h}	6.14 (^2A_u)		yes
Mg(TMP)	D_{2d}	6.39 ($^2B_2$)	6.81 ($^2B_1$)	
	C_2	6.38 (^2A)		no
Zn(TPP)	D_{4h}	6.55 ($^2A_{2u}$)	6.69 ($^2A_{1u}$)	
	C_{4h}	6.54 (^2A_u)		yes
Zn(TDCPP)	D_{4h}	6.68 ($^2A_{2u}$)	6.78 ($^2A_{1u}$)	
	C_{4h}	6.62 (^2A_u)		yes
Ni(TPP)	D_{4h}	6.62 ($^2A_{2u}$)	6.67 ($^2A_{1u}$)	
	D_{2d}	6.51 ($^2B_2$)	6.68 ($^2B_1$)	
	C_{4h}	6.59 (^2A_u)		yes
Ni(TPFPP)	D_{4h}	7.48 ($^2A_{1u}$)	7.58 ($^2A_{2u}$)	
	C_{4h}	7.46 (^2A_u)		yes
Zn(TPFPP)	D_{4h}	7.49 ($^2A_{1u}$)	7.50 ($^2A_{2u}$)	
	C_{4h}	7.47 (^2A_u)		yes
Zn(OClP)	D_{4h}	7.50 ($^2A_{1u}$)	7.58 ($^2A_{2u}$)	
	C_{4h}	7.47 (^2A_u)		yes
Zn(OFP)	D_{4h}	7.75 ($^2A_{1u}$)5	7.79 ($^2A_{2u}$)	
	C_{4h}	7.70 (^2A_u)		yes

[a] The last column indicates whether there is bond length alternation in the case of the C_{4h} structures.

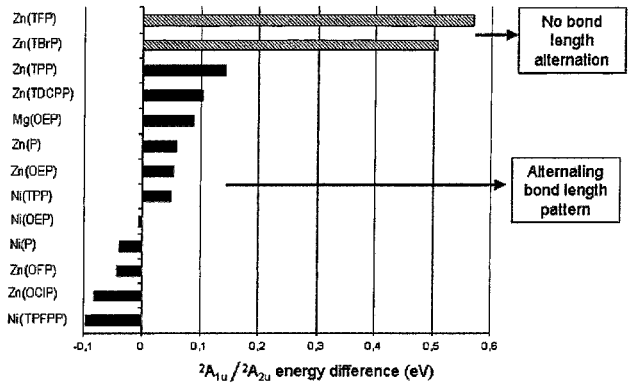

Figure 1. The $^2A_{1u}/^2A_{2u}$ energy difference (eV) for the various D_{4h} symmetry-constrained optimized structures.

geometry optimizations was performed on each porphyrin, for the neutral state and the lowest energy cationic state, with a symmetry constraint, usually C_{4h}, that would permit a pJT-type bond length alternation. Table 2 presents the energetics of the various optimized structures and also indicates which structures exhibit bond length alternation; Figure 1 presents a more "visual" depiction of the same results.

As expected, the neutral metalloporphyrins do not exhibit any bond length alternation while most of the cation radicals do exhibit a pJT-type symmetry-breaking. The data in Table 2 show that the energy difference between the $^2A_{1u}$ and $^2A_{2u}$ cation states, both optimized under D_{4h} symmetry constraints, correlates well with whether the symmetry-relaxed cation adopts a structure with alternating bond lengths or not. This is not surprising

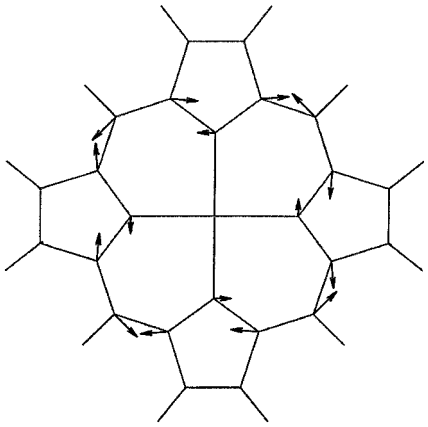

Figure 2. Schematic diagram of the vibrational mode corresponding to the 1789i cm^{-1} (a_{2u}) imaginary frequency of $[Zn(P^{\bullet})]^+$ (D_{4h}).

because the near-degeneracy of the porphyrin HOMOs is the basis for pJT distortions in the cation radicals. On the basis of the calculated results in Table 2, it appears that the difference in energy between the $^2A_{1u}$ and $^2A_{2u}$ cationic states (optimized in D_{4h}) must be less than about 0.15 eV for the π-cation radical to adopt a pJT-type symmetry-broken structure. For $[Mg(TMP^{\bullet})]^+$,[48] $[Zn(TFP^{\bullet})]^+$,[15,49] and $[Zn(TBrP^{\bullet})]^+$ this energy difference is above the threshold and the molecules do not break symmetry on lowering of the symmetry constraint imposed on the optimizations. In contrast, a C_{4h} geometry optimization of $[Zn(TPP^{\bullet})]^+$, for which the $^2A_{1u}/^2A_{2u}$ energy difference has the approximate threshold value of 0.14 eV, results in a symmetry-broken structure with bond length alternation.[50] The cation radicals of metallo-porphine, -OEP, -TDCPP, and -TPFPP derivatives, for which the $^2A_{1u}/^2A_{2u}$ energy difference is clearly below 0.15 eV, also adopt symmetry-broken structures.

How much energy is associated with desymmetrization to an alternant pJT-distorted structure relative to a symmetry-unbroken structure? A fair range of energy gains are associated with this desymmetrization across the various molecules studied. For example, the D_{4h} optimized structures and the C_{4h} pJT-distorted geometries of $[Ni(P^{\bullet})]^+$, $[Zn(OEP^{\bullet})]^+$ and $Zn(TPP^{\bullet})]^+$ are essentially equienergetic.[50] In contrast, the C_{4h} pJT-distorted geometries of $[Ni(OEP^{\bullet})]^+$ and $Ni(TPP^{\bullet})]^+$ are more stable than their respective undistorted D_{4h} structures by a more substantial margin of 0.03−0.04 eV.

Given the small energies associated with the symmetry-breaking distortions, we wished to verify via frequency analyses the nature of the undistorted and symmetry-broken optimized structures. At this point, we have succeeded in accomplishing a vibrational analysis on only the D_{4h} optimized geometry of $[Zn(P^{\bullet})]^+$. For this purpose, we used the B3LYP functional, the LANL2DZ basis set, an "ultrafine grid", and the Gaussian98 program system.[51] The calculation revealed a single a_{2g} imaginary frequency of 1789i cm^{-1} and the corresponding vibrational mode is depicted in Figure 2. This is clearly the vibrational mode along which the pJT distortion occurs and the D_{4h} optimized structure may be regarded as a transition state on the reaction path connecting two degenerate C_{4h} minima.

(48) *meso*-Tetraalkylporphyrins yield A_{2u}-type π-cation radicals.[10]
(49) Ghosh, A. *J. Phys. Chem.* **1994**, *98*, 11004
(50) A linear transit calculation between the D_{4h} and C_{4h} optimized geometries of $Zn(TPP^{\bullet})]^+$ revealed an energy hump, suggesting the possibility of multiple potential energy minima.

Table 3. Selected DFT(PW91/TZP) Optimized Distances (Å)[a]

molecule	symmetry constraint used	M–N	C_α–N (1)	C_α–N (2)	C_α–C_m (1)	C_α–C_m (2)	C_β–C_β	C_α–C_β (1)	C_α–C_β (2)
Zn(P)	C_{4h}	2.0569	1.3735	1.3734	1.3977	1.3978	1.3659	1.4449	1.4450
$[Zn(P^\bullet)]^+$ (^2A_u)	C_{4h}	2.0567	1.3579	1.3849	1.4187	1.3851	1.3634	1.4475	1.4469
$[Zn(P)]^{2+}$	C_{4h}	2.0546	1.3395	1.4030	1.4455	1.3671	1.3567	1.4587	1.4567
Ni(P)	C_{4h}	1.9695	1.3812	1.3812	1.3795	1.3796	1.3599	1.4381	1.4382
$[Ni(P^\bullet)]^+$ (^2A_u)	C_{4h}	1.9651	1.3642	1.3925	1.3984	1.3651	1.3535	1.4471	1.4460
Zn(TFP)	C_{4h}	2.0554	1.3745	1.3745	1.3960	1.3959	1.3693	1.4385	1.4385
$[Zn(TFP^\bullet)]^+$ (^2A_u)	C_{4h}	2.0597	1.3708	1.3713	1.4042	1.4039	1.3704	1.4357	1.4360
Zn(TBrP)	C_{4h}	2.0623	1.3798	1.3800	1.4029	1.4024	1.3622	1.4405	1.4402
$[Zn(TBrP^\bullet)]^+$ (^2A_u)	C_{4h}	2.0661	1.3768	1.3769	1.4106	1.4104	1.3626	1.4381	1.4379
Zn(OEP)	C_{4h}	2.0749	1.3749	1.3747	1.3982	1.3981	1.3807	1.4552	1.4547
$[Zn(OEP^\bullet)]^+$ (^2A_u)	C_{4h}	2.0713	1.3617	1.3851	1.3856	1.4189	1.3821	1.4544	1.4582
Ni(OEP)	C_{4h}	1.9940	1.3822	1.3821	1.3817	1.3815	1.3741	1.4490	1.4487
$[Ni(OEP^\bullet)]^+$ (^2A_u)	C_{4h}	1.9874	1.3672	1.3929	1.3666	1.4006	1.3719	1.4525	1.4577
Mg(OEP)	C_{4h}	2.0792	1.3733	1.3730	1.3999	1.4001	1.3806	1.4539	1.4533
$[Mg(OEP^\bullet)]^+$ (^2A_u)	C_{4h}	2.0747	1.3588	1.3858	1.3852	1.4218	1.3806	1.4548	1.4583
Mg(TMP)	C_2	2.0627	1.3786	1.3780	1.4113	1.4107	1.3644	1.4440	1.4433
$[Mg(TMP^\bullet)]^+$ (^2A)	C_2	2.0649	1.3767	1.3751	1.4193	1.4170	1.3641	1.4415	1.4408
Zn(TPP)	C_{4h}	2.0495	1.3767	1.3763	1.4059	1.4055	1.3640	1.4443	1.4439
$[Zn(TPP^\bullet)]^+$ (^2A_u)	C_{4h}	2.0499	1.3879	1.3618	1.4289	1.3941	1.3624	1.4450	1.4458
Zn(TDCPP)	C_{4h}	2.0487	1.3747	1.3746	1.4047	1.4041	1.3628	1.4437	1.4441
$[Zn(TDCPP^\bullet)]^+$ (^2A_u)	C_{4h}	2.0484	1.3874	1.3587	1.4287	1.3904	1.3601	1.4464	1.4471
Ni(TPP)	C_{4h}	1.9632	1.3845	1.3844	1.3880	1.3877	1.3575	1.4376	1.4372
$[Ni(TPP^\bullet)]^+$ (^2A_u)	C_{4h}	1.9629	1.3972	1.3682	1.4111	1.3753	1.3545	1.4410	1.4423
Ni(TPP)	C_2	1.9600	1.3844	1.3841	1.3884	1.3883	1.3580	1.4375	1.4384
$[Ni(TPP^\bullet)]^+$ (^2A)	C_2	1.9611	1.3688	1.3947	1.3759	1.4097	1.3555	1.4413	1.4403
Ni(TPFPP)	C_{4h}	1.9650	1.3824	1.3818	1.3868	1.3865	1.3558	1.4379	1.4370
$[Ni(TPFPP^\bullet)]^+$ (^2A_u)	C_{4h}	1.9609	1.3951	1.3666	1.4061	1.3736	1.3502	1.4458	1.4459
Zn(TPFPP)	C_{4h}	2.0529	1.3747	1.3743	1.4050	1.4048	1.3618	1.4448	1.4441
$[Zn(TPFPP^\bullet)]^+$ (^2A_u)	C_{4h}	2.0506	1.3889	1.3572	1.4293	1.3884	1.3578	1.4510	1.4497
Zn(OClP)	C_{4h}	2.0573	1.3744	1.3744	1.3921	1.3921	1.3678	1.4458	1.4460
$[Zn(OClP^\bullet)]^+$ (^2A_u)	C_{4h}	2.0516	1.3854	1.3603	1.3784	1.4107	1.3666	1.4525	1.4572
Zn(OFP)	C_{4h}	2.0544	1.3767	1.3765	1.3934	1.3934	1.3606	1.4401	1.4401
$[Zn(OFP^\bullet)]^+$ (^2A_u)	C_{4h}	2.0515	1.3593	1.3893	1.4157	1.3782	1.3601	1.4513	1.4481

[a] The symbols (1) and (2) generally refer to "short" and "long", where relevant.

(c) Geometrical Aspects of the pJT Distortions. Table 3 presents key optimized geometry parameters of the metalloporphyrin cations studied, the corresponding parameters for the neutral metalloporphyrins being given in Table S1 in the Supporting Information. Table 4 lists the average, experimental $C_\alpha-N$ and $C_{meso}-C_\alpha$ distances for crystallographically characterized metalloporphyrin cation radicals, as obtained from the Cambridge Crystallographic Database (CSD). Nearly all the optimized C_{4h} ^2A_u cation radicals exhibit a significant bond length alternation around the central 16-membered $C_{12}N_4$ ring. Figure 3 illustrates this alternant bond length distribution for $[Zn(P^\bullet)]^+$ and for the dication $[Zn(P)]^{2+}$, with "long" and "short" bonds indicated as L and S, along with experimentally obtained bond lengths for relevant molecules.

How do the calculated degrees of bond length alternation compare with experiment? According to the results shown in Figure 3, theory and experiment appear to be in good agreement. We examined whether there might be some correlation between the $^2A_{1u}/^2A_{2u}$ energy difference under D_{4h} symmetry and the degree of bond length alternation when the symmetry is relaxed to C_{4h}. Interestingly, based on our calculated results (Table 3), no such correlation is apparent. For the calculated alternant structures, the differences between the long and short bonds are 0.025 and 0.020 Å for the $C_{meso}-C_\alpha$ and $C_\alpha-N$ bonds, respectively, and the average deviations, across all the optimized structures, are only 0.0017 and 0.0016 Å, respectively. In other words, metalloporphyrin π-cation radicals appear to undergo a certain fixed amount of pJT distortion or none at all. Figure 4 depicts this idea graphically via a scatter plot of bond length alternation parameters versus the $^2A_{1u}/^2A_{2u}$ energy difference.

Of the crystallographically characterized structures listed in Table 4, eight exhibit a clear, alternant bond length distribution. However, certain of the structures exhibit an alternant pattern for only part of the central 16-membered $C_{12}N_4$ ring. Thus, except for the eight clearly alternant cases listed in Table 4, the descriptors L an S in Table 4 are not necessarily particularly meaningful: The bond lengths shown in Table 4 are simply averaged over alternating, as opposed to adjacent, bonds in the macrocycle.

Another feature of interest is that an alternant geometry may coexist with other distortions of the porphyrin framework, such as ruffling or saddling.[26] For example, the C_2 optimized geometry of $[Ni(TPP^\bullet)]^+$ is ruffled, with a ruffling torsion angle of 12.3°, and exhibits the same degree of bond length alternation as the planar geometry obtained with a C_{4h} symmetry constraint.

Finally, the case of $[Zn(TPP^\bullet)]ClO_4$ deserves some comment. A crystal structure reported by Scheidt and co-workers

(51) Frisch, M. J.; Trucks, G. W.; Schlegel, H. B.; Scuseria, G. E.; Robb, M. A.; Cheeseman, J. R.; Zakrzewski, V. G.; Montgomery, J. A., Jr.; Burant, J. C.; Dapprich, S.; Millam, J. M.; Daniels, A. D.; Kudin, K. N.; Strain, M. C.; Farkas, O.; Tomasi, J.; Barone, V.; Cossi, M.; Cammi, R.; Mennucci, B.; Pomelli, C.; Adamo, C.; Clifford, S.; Ochterski, J.; Petersson, G. A.; Ayala, P. Y.; Cui, Q.; Morokuma, K.; Malick, D. K.; Rabuck, A. D.; Raghavachari, K.; Foresman, J. B.; Cioslowski, J.; Ortiz, J. V.; Stefanov, B. B.; Liu, G.; Liashenko, A.; Piskorz, P.; Komaromi, I.; Gomperts, R.; Martin, R. L.; Fox, D. J.; Keith, T.; Al-Laham, M. A.; Peng, C. Y.; Nanayakkara, A.; Gonzalez, C.; Challacombe, M.; Gill, P. M. W.; Johnson, B.; Chen, W.; Wong, M. W.; Andres, J. L.; Gonzalez, C.; Head-Gordon, M.; Replogle, E. S.; Pople, J. A. *Gaussian*, Revision A.5; Gaussian, Inc.: Pittuburgh, PA, 1998.

Table 4. Average Bond Distances (Å) for Metalloporphyrin π-Cation Radicals and Mixed-Valence π-Cation Radicals, As Available from the Cambridge Structural Database (CSD) during April 1998[b]

	C_α–N		C_α–C_m			
molecule	(1)	(2)	(1)	(2)	CSD	ref
$[Cu^{II}(TPP^{\bullet})](SbCl_4)$	1.395(12)	1.380(11)	1.413(20)	1.388(11)	bosbam10	27
$[Zn(TPP^{\bullet})](ClO_4)$	1.380(2)	1.364(2)	1.426(5)	1.400(4)	savlik01	28
$[CuII(OETPP^{\bullet})](ClO_4)$	1.395(4)	1.372(6)	1.421(6)	1.393(3)	lidtoh	29
$[Zn(TPP^{\bullet})](ClO_4)$	1.364(9)	1.361(6)	1.415(9)	1.409(4)	savlik	28
$[FeIII(TPP^{\bullet})(ClO_4)](ClO_4)$	1.371(16)	1.382(35)	1.436(9)	1.420(4)	bubfaf10	30
$[FeIII(TTP^{\bullet})Cl][SbCl_6]$	1.387(5)	1.387(11)	1.398(3)	1.382(6)	dopbal10	31
$[Zn(TPP^{\bullet})](ClO_4)$	1.349(12)	1.362(15)	1.410(11)	1.394(9)	ptppzn	39
$[Cu^{II}(OETPP^{\bullet})]I_7$	1.329(47)	1.354(59)	1.456(38)	1.398(52)	lidtun	29
$[Mg(TPP^{\bullet})](ClO_4)$	1.371(5)	1.380(5)	1.411(10)	1.408(8)	boyfaw	32
$[Cu^{II}(TMesP^{\bullet})](SbCl_6)$[a]	1.368(6)	1.356(4)	1.392(8)	1.400(10)	sebxec	17
$[Zn(OEP^{\bullet})(H_2O)](ClO_4)$	1.384(3)	1.341(3)	1.417(1)	1.372(2)	sebxig10	16
$[CuII(TMesP^{\bullet})]_2[ReO_4]$[a]	1.393(0)	1.365(7)	1.407(9)	1.383(7)	jilgam	33
$[Fe^{III}(OEP^{\bullet})Cl][ClO_4]$	1.391(5)	1.356(3)	1.407(3)	1.372(1)	jovriv10	34
$[Mg(OEP^{\bullet})(EtOH)]$-$[Mg(OEP^{\bullet})(ClO_4)]ClO_4$	1.387(8)	1.343(8)	1.420(8)	1.367(8)	rijmec	35
$[FeIIi(OEP^{\bullet})(ClO_4)_2$	1.376(2)	1.373(0)	1.385(1)	1.380(3)	jovrer	36
$[Mg(OEP^{\bullet})(ClO_4)$	1.370(3)	1.361(3)	1.393(7)	1.390(5)	rijmig	35
$[NiII(OEP^{\bullet/2})]_2[SbCl_6]$	1.382(8)	1.368(15)	1.379(10)	1.364(12)	pavkec10	37
$[(Zn(OEP^{\bullet/2})\ (H_2(OEP^{\bullet/2})]\ (SbCl_6)$	1.365(5)	1.368(1)	1.394(3)	1.391(5)	relguk	37
$[Cu^{II}(OEP^{\bullet/2})]_2[SbCl_6]$	1.380(7)	1.372(5)	1.372(9)	1.378(10)	pavkig10	37

[a] TMesP = *meso*-tetramesitylporphyrinato. [b] Average deviations are given in parentheses.

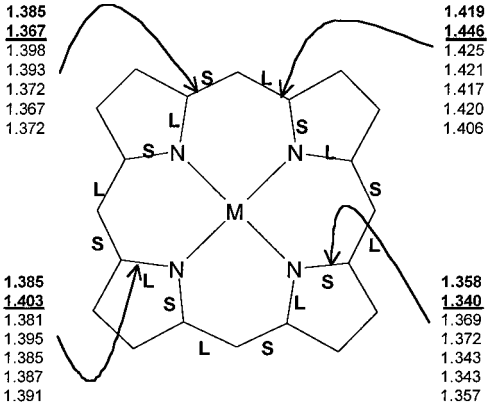

Figure 3. Carbon−carbon and carbon−nitrogen bond distances (Å) along the central $C_{12}N_4$ ring of metalloporphyrin cations. Optimized distances from this work are shown in bold, relevant crystallographic numbers being shown as plain text. From top to bottom, within each box, the numbers refer to $[Zn(P^{\bullet})]^+$ (^2A_u; C_{4h}), $[Zn(P)]^{2+}$ (^1A_g; C_{4h}), $[Zn(TDCPP^{\bullet})(ClO_4)]$,[38] $[Cu^{II}(OETPP^{\bullet})](ClO_4)$,[29] $[Zn(OEP^{\bullet})(H_2O)](ClO_4)$,[16] $[Mg(OEP^{\bullet})(EtOH)][Mg(OEP^{\bullet})(ClO_4)](ClO_4)$,[35] and $[Fe(III)(OEP^{\bullet})Cl]ClO_4$.[34] The symbols "S" and "L" indicate short and long bonds, respectively.

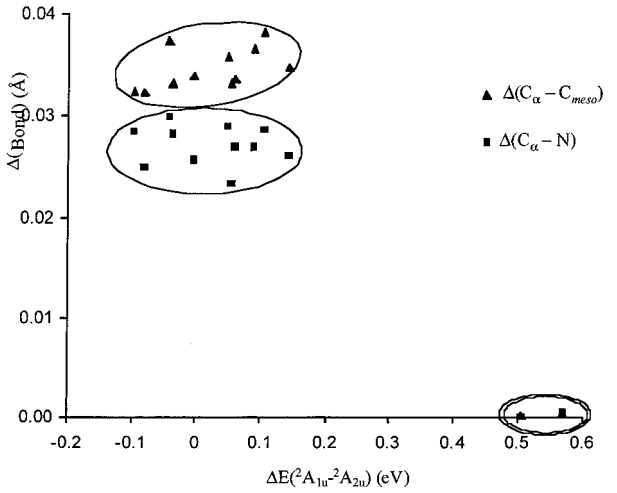

Figure 4. Scatter plot of the calculated $C_\alpha-C_{meso}$ and $C_\alpha-N$ bond distance alternations for C_{4h} pJT-distorted cation radicals versus the $^2A_{1u}/^2A_{2u}$ energy difference for the respective D_{4h} symmetry-constrained structures.

revealed two symmetry-distinct structures of this cation, one alternant (CSD code SAVLIK01) and the other not (CSD code SAVLIK).[26] This may be related to our finding (see above) that the alternant and nonalternant structures of $[Zn(TPP^{\bullet})]^+$ are essentially equi-energetic.

(d) Spin Density Profiles. Spin density profiles were evaluated for the $^2A_{1u}$ (D_{4h}), $^2A_{2u}$ (D_{4h}), and ^2A_u (C_{4h}) states of selected molecules, viz. Ni(P), Zn(P), Zn(TPP), and Ni(OEP), by means of spin-unrestricted calculations on the corresponding optimized geometries (Table 5). As expected, the spin density profiles of all these molecules were found to be somewhere between A_{1u}- and A_{2u}-type. This is shown in Figure 5, which depicts the open-shell MO of $[Zn(P^{\bullet})]^+$. An important result is that although the structural results described so far tend to blur the distinction between A_{1u}- and A_{2u}-type radicals, it *is* nevertheless possible to describe the spin density profile in each case studied as more A_{1u}-like than A_{2u}-like or vice versa. The C_{4h} forms of both $[Ni(P^{\bullet})]^+$ and $[Ni(OEP^{\bullet})]^+$ exhibit relatively small spin populations on the nitrogens, modest spin populations on the meso carbons, and large spin populations on certain α and β carbons. In other words, the spin density profile is relatively A_{1u}-like. In contrast, $[Zn(P^{\bullet})]^+$ and $[Zn(TPP^{\bullet})]^+$ exhibit large spin populations on the nitrogens and meso carbons but small spin populations on the α and β carbons, i.e., a relatively A_{2u}-like spin density profile. Based on correlating these results with the energetics information given in Table 2, it appears that whether a pJT-distorted metalloporphyrin cation radical exhibits an a_{1u}- or a_{2u}-like spin density profile is intimately related to the relative stability of the $^2A_{1u}$ and $^2A_{2u}$ states in the absence of pJT symmetry-breaking. Thus, although the rule of thumb that metallo-OEP derivatives yield A_{1u} radicals while metallo-TPP derivatives yield A_{2u} radicals is simplistic (in that it neglects the fairly ubiquitous pJT distortions), it is correct in an approximate sense. These results may further imply that even with respect to various spectroscopic properties that we have not explicitly addressed in this study such as resonance Raman marker band frequencies, metallo-OEP radicals may exhibit

Table 5. Atomic Spin Populations of the $^2A_{1u}$, $^2A_{2u}$, and ^2A_u Cation Radical States for Selected Metalloporphyrins

					C_α			C_β	
molecule	point group	SOMO[a]	metal	N	(1)	(2)	C_{meso}	(1)	(2)
$[Ni(P^\bullet)]^+$	D_{4h}	a_{1u}	−0.018	−0.035	0.146		−0.051	0.026	
	D_{4h}	a_{2u}	−0.004	0.084	−0.038		0.242	0.008	
	C_{4h}	a_u	−0.012	0.011	0.116	0.043	0.052	0.058	−0.020
$[Zn(P^\bullet)]^+$	D_{4h}	a_{1u}	0.003	−0.036	0.147		−0.054	0.024	
	D_{4h}	a_{2u}	0.013	0.090	−0.041		0.248	0.003	
	C_{4h}	a_u	0.011	0.058	−0.023	0.042	0.163	0.041	−0.023
$[Zn(TPP^\bullet)]^+$	D_{4h}	a_{1u}	0.003	−0.034	0.141		−0.052	0.021	
	D_{4h}	a_{2u}	0.019	0.078	−0.036		0.221	0.009	
	C_{4h}	a_u	0.014	0.067	−0.038	0.016	0.187	0.032	−0.019
$[Ni(OEP^\bullet)]^+$	D_{4h}	a_{1u}	−0.014	−0.034	0.149		−0.053	0.018	
	D_{4h}	a_{2u}	−0.004	0.061	−0.038		0.233	0.021	
	C_{4h}	a_u	−0.010	0.010	0.102	0.032	0.070	0.067	−0.029

[a]SOMO = singly occupied MO.

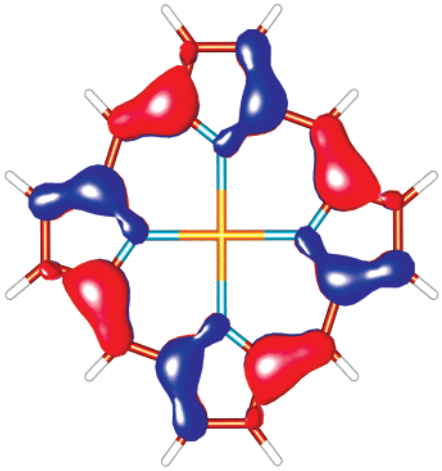

Figure 5. The a_u singly occupied MO of pJT-distorted $[Zn(P^\bullet)]^+$ (C_{4h}).

predominant A_{1u} character and metallo-TPP radicals predominant A_{2u} character, consistent with traditional ideas.[14] These results are also consistent with the current consensus[2] among experimentalists that peroxidase compound I intermediates (such as HRP-I[3] and CPO-I[4]), where the porphyrin is "OEP-like", feature A_{1u}-type, rather than A_{2u}-type, porphyrin radicals.

(e) Cofacial Dimers of Metalloporphyrin Radicals. Many of the metalloporphyrin π-cation radicals that have been structurally characterized exist as cofacial, sometimes laterally shifted, dimers in the crystalline phase. Accordingly, the question naturally arises as to whether the observed alternant structures reflect a pJT distortion or are a result of the dimerization. Scheidt addressed this question by solving the crystal structure of a sterically hindered nondimerizing $[Zn\{TDCPP^\bullet\}]^+$ derivative;[22] the structure was clearly alternant, strengthening the case for a pJT distortion, consistent with our own computational findings (Table 2).[52] Bocian and co-workers have also provided EPR and Raman evidence of an A_{1u}/A_{2u} mixed state for the $[Zn\{TDCPP^\bullet\}]^+$ radical.[20] Nevertheless, we have examined the structures and symmetries of the cofacial dimers, $[\{Zn(P)\}_2]^{0,+,2+}$, via DFT geometry optimizations.

The relative orientation of porphyrin dimers is described by a number of parameters such as the lateral shift (i.e. the offset of the metal centers) and the angle by which the two porphyrins are rotated with respect to each other (which can be defined as the smallest N−M−M′−N′ torsion angle, where M and M′ are the metal ions and N and N′ are the pyrrole nitrogens in the two rings). In addition, the alternant porphyrin rings also have a sense of directionality,[53] which adds another degree of freedom to this issue. In this study, we have not addressed the issue of laterally offset porphyrin dimers; otherwise, Table 6 summarizes the various molecular symmetries examined for the cofacial species, $[\{Zn(P)\}_2]^{0,+,2+}$.

Table 6 also presents the energetics of the different conformations of Zn(P) dimer for the neutral, monocationic, and dicationic oxidation levels. For the neutral dimer, the question of ring directionality of the individual porphyrins does not arise and the staggered conformation of the dimer is very slightly favored over an eclipsed conformation. For $[\{Zn(P)\}_2]^+$ and $[\{Zn(P)\}_2]^{2+}$, the individual porphyrin rings do, in general, exhibit alternant geometries and the question of relative directionality of the two rings is a relevant issue. Table 6 shows that ring directionality has little impact on the energetics of $[\{Zn(P)\}_2]^+$ and that the staggered conformation is again very slightly favored over the eclipsed conformation. Only for $[\{Zn(P)\}_2]^{2+}$ is there a clear and substantial preference for the staggered conformation and, within this conformation, there is a certain preference for the two porphyrin rings to exhibit the same sense of cyclic directionality.

Table S1 (Supporting Information) presents selected optimized bond distances for the different dimer conformations and oxidation states studied and Table S2 (Supporting Information) presents various inter-ring separations and the relative rotation of the two rings in the dimers. Except for conformation II, all the conformations of $[\{Zn(P)\}_2]^{2+}$ exhibit alternant porphyrin ring geometries, almost identical to monomeric $[Zn(P^\bullet)]^+$. It is not clear why conformation II does not exhibit a significant bond length alternation.

The optimized structural parameters of $[Zn(P^\bullet)]_2^{2+}$ rather closely resemble those found in the crystal structure of the $[Zn(OEP^\bullet)(H_2O)]ClO_4$ dimer reported by Song et al.[16] The experimentally studied dimer exhibits no lateral shift and the two porphyrin rings in the dimer are rotated 31.3° relative to each other. The crystal structure[16] exhibits a clear, alternant bond length distribution and the two rings in the dimer have opposite

(52) This may explain why the A_{1u} versus A_{2u} character of the $[Zn\{TDCPP^\bullet\}]^+$ cation has been controversial: (a) Barzilay, C. M.; Sibilia, S. A.; Spiro, T. G.; Gross, Z. *Chem. Eur. J.* **1995**, *1*, 222. (b) Vangberg, T.; Ghosh, A. *J. Am. Chem. Soc.* **1998**, *120*, 6227. Our views on the $[Zn\{TDCPP^\bullet\}]^+$ cation are most consistent with ref 17.

(53) For a formal definition of cyclic directionality, see: Mislow, K. *Chimia* **1986**, *40*, 395. For a recent discussion, see: Ghosh, A. *Theor. Chem. Acc.* **2000**, *104*, 157. Very briefly, a cycle is made of any three noncollinear points. A directed cycle is one that is *not* bisected by a mirror plane or a C_2 axis.

Table 6. Description of Different Conformations Studied for the Zn(P) Dimer Derivatives, $[\{Zn(P)\}_2]^{0,+,2+}$ (relative energies (eV) shown in columns 4−6 refer to conformation III as the zero level)

conformation	point group	cyclic directionality	initial relative twist of porphyrin rings	$[\{Zn(P)\}_2]^0$	$[\{Zn(P)\}_2]^+$	$[\{Zn(P)\}_2]^{2+}$
I	C_{4h}	same	0° [a]	0.019	0.011	0.042
II	D_4	opposite	0°	0.015	0.038	0.170
III	D_4	opposite	22.5°	0.000	0.000	0.000
IV	C_4	same	22.5°	−0.001	−0.010	0.001

[a] The symmetry constraint prevents this twist angle from changing under geometry optimization.

cyclic directionalities. Thus, the experimental structure[16] most closely resembles conformation III, described in Table 5. The optimized inter-ring twist angle in conformation III of $[Zn(P^{\bullet})]_2^{2+}$ is 24.8°, 6.5° less than the analogous value in the crystal structure. The optimized inter-ring separations for $[Zn(P^{\bullet})]_2^{2+}$ also agree rather well with the crystal structure (although, because of the axial water ligand, the Zn atom is raised 0.24 Å over the mean porphyrin plane). The experimental Zn···Zn distance in the dimer is 3.79 Å,[16] which may be compared to a value of 3.73 Å for conformation III of $[Zn(P^{\bullet})]_2^{2+}$ (Table 8). The separation between the 24-atom mean planes of the two porphyrin rings is 3.31 Å for the experimentally studied $[Zn(OEP^{\bullet})]_2^{2+}$,[16] compared to an optimized value of 3.78 Å for $[Zn(P^{\bullet})]_2^{2+}$. In view of the fact that the $[Zn(P^{\bullet})]_2^{2+}$ dication is only a very approximate model of the species studied crystallographically, the agreement between theory and experiment may be regarded as quite good.

The delocalized, mixed-valence π-cation radical $[Zn(P^{\bullet/2})]_2^+$ exhibits alternant porphyrin ring geometries in conformations I, II, and IV, but the degree of bond length alternation is about half that found for $[Zn(P^{\bullet})]_2^{2+}$. The smaller bond length alternations are in agreement with the crystallographic structure[35] of the $[Ni(OEP^{\bullet/2})]_2^+$ cation (Table 4) where the short and long $C_\alpha-N$ and $C_\alpha-C_m$ bonds both differ by 0.014 Å, in reasonable agreement with a difference of 0.014 Å for the $C_\alpha-N$ bonds and a difference of 0.018 Å for the $C_\alpha-C_m$ bonds, respectively, in the optimized structures of $[Zn(P^{\bullet/2})]_2^+$.

Finally, a few words may be of interest with regard to the inter-ring orbital interactions in the dimeric radicals. Figure 6 depicts the LUMO, HOMO, HOMO-1, and HOMO-2 from a spin-restricted DFT calculation on conformation III of $[Zn(P^{\bullet})]_2^{2+}$. Note that certain of these "supermolecule" MOs, viz. the HOMO-1 and HOMO-2, exhibit bonding interactions between "a_u" frontier MOs on the individual rings. Moreover, note that the supermolecule MOs HOMO-1 and LUMO are very similar in shape except that the former involves intermonomer bonding interactions and the latter involves intermonomer antibonding interactions. The same applies to the HOMO and HOMO-2 (Figure 6) but because both of these are doubly occupied MOs, they do not contribute significantly to inter-ring bonding. In other words, the porphyrin rings in the dimer radicals are held together by net covalent bonding interactions, in addition to other possible interactions.

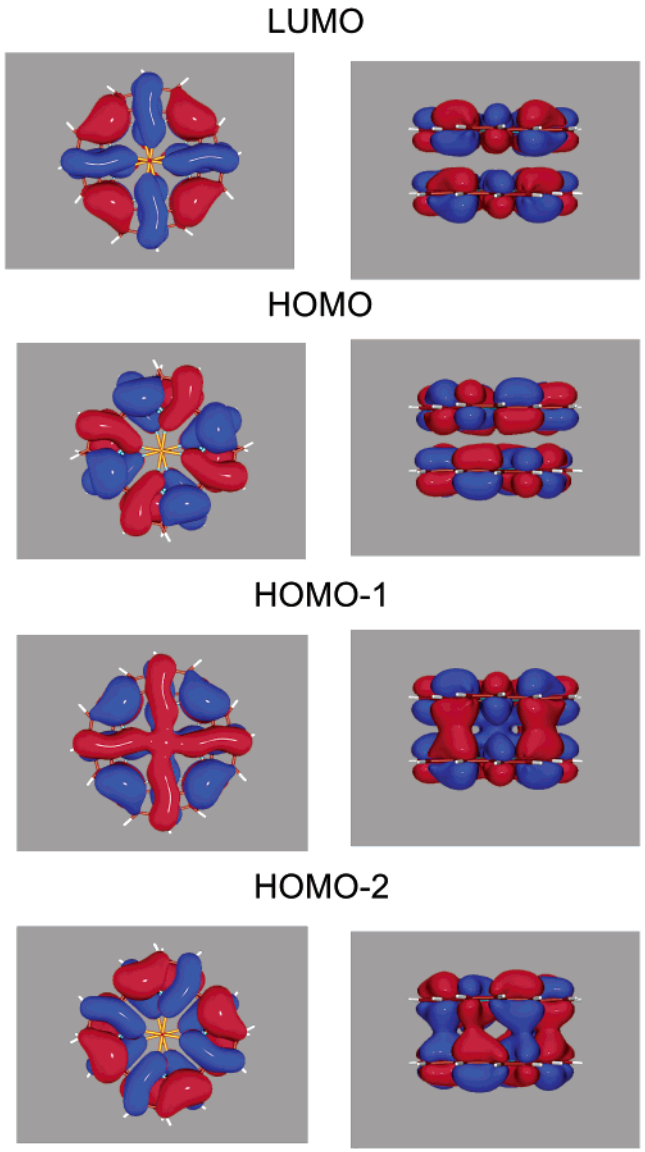

Figure 6. Top and side views of the LUMO, HOMO, HOMO-1, and HOMO-2 of conformation III of $[Zn(P^{\bullet})]_2^{2+}$ obtained from a spin-restricted DFT calculation.

Conclusions

The principal conclusions from this study may be enumerated as follows.

(1) More than a decade ago, Prendergast and Spiro[15] suggested, on the basis of vibrational spectroscopy and semiempirical calculations, that certain metalloporphyrin π-cation radicals exhibit a spontaneous symmetry-breaking and exhibit a significant bond length alternation along the central $C_{12}N_4$ ring. Over the past decade, however, it has become clear that semiempirical calculations do not provide a correct description of the potential energy surfaces of porphyrins. The crystallographic evidence in favor of the symmetry-breaking distortions, while persuasive, is still replete with ambiguities and is not quite conclusive. Under these circumstances, we hoped that nonlocal DFT calculations would allow us to determine whether the symmetry-breaking distortions proposed by Prendergast and Spiro[15] really exist. The results provide strong evidence that such distortions do occur for many but not all metalloporphyrin π-cation radicals.

(2) Whether a pJT distortion takes place is directly related to whether the difference in energy between the A_{1u} and A_{2u} radicals, optimized under nonsymmetry-breaking constraints, is below a certain threshold (0.15 eV). This leads us to characterize this distortion as a pJT effect.

(3) According to the threshold criterion, we predict that metalloporphine and metallo-OEP radicals should generally be pJT-distorted and metallo-*meso*-tetrahalogenoporphyrin and metallo-*meso*-tetramethylporphyrin radicals should not. For $[Zn(TPP^{\bullet})]^{+}$, the $^2A_{1u}/^2A_{2u}$ energy difference is almost exactly at the threshold of 0.15 eV, apparently consistent with the experimental observation[26] of both symmetry-broken and undistorted structures for this species.

(4) Although most of the radicals studied are accurately described as ^2A_u with reference to the C_{4h} point group, *the spin density profile can generally be described as either A_{1u}- or A_{2u}-like*. In terms of the spin density profile, the calculations do support the rule of thumb that OEP derivatives yield A_{1u}-type radicals while TPP derivatives yield A_{2u}-type radicals. Because biological porphyrin ligands are "OEP-like", this implies that the porphyrin radical in peroxidase compound I intermediates should be A_{1u}-like, consistent with the current consensus of opinion. The $^2A_{1u}/^2A_{2u}$ energy difference, under D_{4h}, appears to be a key determinant of whether a pJT-distorted cation radical is more A_{1u}- or A_{2u}-like in terms of its spin density profile.

(5) Our calculations also indicate that cofacial dimerization of metalloporphyrin radicals has relatively little impact on bond length alternation in the individual rings. An interesting result, consistent with experiment, is that the bond length alternation in the delocalized mixed-valence dimer $[Zn(P^{\bullet/2})]_2^{+}$ is about half that found for $[\{Zn(P^{\bullet})\}_2]^{2+}$.

Acknowledgment. We thank the Norwegian Research Council and the VISTA program of Statoil (Norway) for financial support.

Supporting Information Available: Tables S1 and S2 giving selected "intramonomer" optimized distances and selected interring distances and relative twist of the porphyrin rings for confomations of $[\{Zn(P)\}_2]^{0,+,2+}$, as well as optimized Cartesian coordinates of most of the molecules studied are included (PDF). This material is available free of charge via the Internet at http://pubs.acs.org.

JA011438H